

*Cocoa shell: an industrial by-product
for the preparation of suspensions of
holocellulose nanofibers and fat*

**C. Gómez Hoyos, P. Mazo Márquez,
L. Penagos Vélez, A. Serpa Guerra,
A. Eceiza, L. Urbina, J. Velásquez-Cock,
P. Gañán Rojo, et al.**

Cellulose

ISSN 0969-0239

Cellulose

DOI 10.1007/s10570-020-03222-6




Your article is protected by copyright and all rights are held exclusively by Springer Nature B.V.. This e-offprint is for personal use only and shall not be self-archived in electronic repositories. If you wish to self-archive your article, please use the accepted manuscript version for posting on your own website. You may further deposit the accepted manuscript version in any repository, provided it is only made publicly available 12 months after official publication or later and provided acknowledgement is given to the original source of publication and a link is inserted to the published article on Springer's website. The link must be accompanied by the following text: "The final publication is available at link.springer.com".



ORIGINAL RESEARCH

Cocoa shell: an industrial by-product for the preparation of suspensions of holocellulose nanofibers and fat

C. Gómez Hoyos · P. Mazo Márquez · L. Penagos Vélez · A. Serpa Guerra ·
A. Eceiza · L. Urbina · J. Velásquez-Cock · P. Gañán Rojo · L. Vélez Acosta ·
R. Zuluaga 


Received: 30 November 2019 / Accepted: 8 May 2020

© Springer Nature B.V. 2020

Abstract Cocoa shell (CS) is a by-product of the chocolate industry with limited economic benefit and a high environmental impact. In this study, a new material for the food industry that consists of nanocellulose fibers with CS fat was successfully isolated (yield of approximately 7.12%). The material was characterized with attenuated total reflection–Fourier transform infrared spectroscopy (ATR–FTIR), solid-state ^{13}C nuclear magnetic resonance (^{13}C NMR), X-ray diffraction (XRD), fluorescence and atomic force microscopy (AFM). The XRD, ^{13}C NMR, and ATR–FTIR results suggest that the structure of the cellulosic CS fibers can be interpreted as cellulose I_β . The crystallinity index (CrI) of an isolated sample was investigated by different methods with

ATR–FTIR, ^{13}C NMR, and XRD. According to the results, ^{13}C NMR and XRD are the most adequate methods for quantifying the CrI of cellulosic samples in the presence of fat. In addition, the XRD results indicate that approximately 65 to 70% of the sample was crystalline. According to the fluorescence microscopy results, the cellulosic sample formed a suspension with fat, and the AFM results show that the cellulosic part of the sample had nanometric diameters between 30–80 nm with high aspect ratios. Consequently, a suspension of nanocellulose, hemicellulose, and fat was isolated from CS by chemical and mechanical treatments. The new material can be called a “suspension of holocellulose nanofibers and fat” owing to its composition and fiber diameters. The

C. Gómez Hoyos · J. Velásquez-Cock
Programa de Ingeniería en Nanotecnología, Universidad
Pontificia Bolivariana, Circular 1 N° 70-01,
50031 Medellín, Colombia

P. Mazo Márquez · A. Serpa Guerra · L. Vélez Acosta ·
R. Zuluaga 
Facultad de Ingeniería Agroindustrial, Universidad
Pontificia Bolivariana, Circular 1 N° 70-01,
050031 Medellín, Colombia
e-mail: robin.zuluaga@upb.edu.co

L. Penagos Vélez
Centro de Investigación, Desarrollo y Calidad - CIDCA,
Compañía Nacional de Chocolates S.A.S, Km 2-Vía,
Autopista Medellín-Bogotá, Vía Belén, Rionegro,
Colombia

A. Eceiza · L. Urbina
Grupo “Materiales+Tecnologías”, Escuela de Ingeniería
de Gipuzkoa, Departamento de Ingeniería Química y del
Medio Ambiente, Universidad del País Vasco (UPV/
EHU), Plaza Europa 1, 20018 San Sebastián, Spain

P. Gañán Rojo
Facultad de Ingeniería Química, Universidad Pontificia
Bolivariana, Circular 1 N 70-01, 050031 Medellín,
Colombia

high aspect ratio of the nanocellulose fibers in the suspension resulted in an entangled network that stabilized the CS fat.

Keywords Cocoa shell · Nanocellulose · Cellulose crystallinity index · Cocoa shell fat · Holocellulose nanofibers

Introduction

Cacao (*Theobroma cacao* L.) is the fruit of the cacao tree. Its seeds are commonly called “cocoa beans” and consist of two cotyledons and a small germ. This fruit has been a social and economic alternative to illicit crops in Colombia. Its growing cultivation has been promoted by the global cocoa deficit, caused by the growing demand in Europe and Asia and the climatic changes in African countries. Between 2007 and 2017, the cocoa harvesting area in Colombia increased by approximately 40%, thereby generating employment for 38,000 farming families and 100,000 employments in other sectors of the productive chain (FEDECA-CAO 2019).

Despite its economic and social benefits, the industry uses only 10 wt% of the fresh fruit and produces over 40,000 t waste monthly (Campos-Vega et al. 2018; Lu et al. 2018). For instance, the cocoa shell (CS) represents 12 wt% of the raw material. It is removed together with the germ before or after roasting and is considered an industrial by-product of the cocoa production. Because the Colombian production of cocoa beans was 56,808 t in 2017 (FAOSTAT), Colombia generated approximately 6816 t of this waste type during that year FAO (2019). The waste has been mainly used as fuel for boilers, in the formulation of animal food, and in the manufacture of fertilizers (Okiyama et al. 2017).

Some published studies and patents have suggested alternative applications for this material, which contains very interesting compounds from a nutritional point of view: for instance, phenolic compounds, fibers, and a significant fat content with a lipid profile very similar to that of cocoa butter (El-Saied et al. 1981; Serra Bonvehí and Ventura Coll 1999; Lecumberri et al. 2007; Okiyama et al. 2017). These applications may improve the efficiency of the chocolate productive chain. Furthermore, CS can be

used to produce nanostructures such as vegetable nanocellulose fibers (Souza et al. 2019). Nanocellulose is a nanomaterial extracted from wood, cotton, natural fibers, and different agricultural by-products, such as bananas (Zuluaga et al. 2009), cotton (Chanzy et al. 1978), walnut shells (Hemmati et al. 2018) and tunicate (Jonoobi et al. 2015).

Researchers that study the nanocellulose isolation process from different vegetable resources usually investigate its properties and the influence of the non-cellulosic polysaccharides and their composition. However, they have not considered other important components of vegetable structures (Nelson and O'Connor 1964b; Chanzy et al. 1978; Sugiyama et al. 1991a; Evans et al. 1995; Newman 2004; Sun et al. 2004; Zuluaga et al. 2009; Poletto et al. 2012). Owing to its composition, CS (*Theobroma cacao* L.) might be an alternative source for expanding the sources of nanomaterials: flavonoids, antioxidants, fat, and polyphenols can be added to nanocellulose to provide novel functionalities for food formulations (Donkoh et al. 1991; Martín-Cabrejas et al. 1994; Bonvehí and Jordà 1998; Karim 2014; Okiyama et al. 2017; Lu et al. 2018). Considering the high number of recent publications about the use of nanocellulose as an ingredient in food products, the material could become an active topic in the nanocellulose research field (Gómez et al. 2016). Nanocellulose has been widely used in oil–water emulsions (Dickinson 2012; Winuprasith and Suphantharika 2015) and as a functional ingredient (Gómez et al. 2016), food stabilizer (Ström et al. 2013), and rheological modifier in ice cream (Velásquez-Cock et al. 2019).

To investigate the potential of nanocellulose fibers isolated from CS as a food ingredient, the effects of chemical and mechanical treatments on the nanocellulose composition, structure, and morphology were investigated in this study. The chemical modifications in the sample generated by isolation treatment were analyzed with attenuated total reflection–Fourier transform infrared spectroscopy (ATR–FTIR) and solid-state ^{13}C nuclear magnetic resonance (^{13}C NMR). In addition, X-ray diffraction (XRD) was applied to assess the fiber crystalline structure, while its crystallinity index (CrI) was investigated by different methods with ATR–FTIR, ^{13}C NMR, and XRD. Finally, fluorescence and atomic force microscopy (AFM) was applied to study the morphology of the obtained suspension of nanocellulose and fat.

Materials and methods

The CS of the main varieties of cocoa beans (*Theobroma cacao L.*) cultivated in Colombia were supplied by *Compañía Nacional de Chocolates* after the roasting process. The CS were ground with a Resch mill such that they could pass through a 1 mm screen (Mesh No. 18). Table 1 presents the most relevant chemical components of the CS.

Isolation of cellulose nanofibers

The CS was chemically treated according to the KOH-5 procedure developed by Zuluaga et al. (2009) to remove non-cellulosic components. First, the CS was vigorously stirred at room temperature for 14 h with 5 wt% KOH solution. Then, the insoluble residue was delignified with 1 wt% NaClO₂ at pH 5.0 and adjusted with 10 wt% acetic acid at 70 °C for 1 h. A second treatment with KOH solution under the same conditions as in the first step was used. Finally, a 1 wt% HCl solution was added and treated at 80 °C for 2 h to remove mineral traces. In each treatment step, the insoluble residue was extensively washed with distilled water until the pH was neutral. Finally, the cellulosic material (2 wt%) was passed 30 times through a grinder (Masuko Sangyo, Supermasscolloider) according to the G30 procedure developed by (Velásquez-Cock et al. 2016). The overall process has a yield of approximately 7.12%.

Finally, suspensions of 0.1 wt% CS nanocellulose (CSNC) were vacuum-filtered through a 0.2 μm nylon

membrane. The resulting films were oven-dried at 40 °C for 72 h and stored for the ATR–FTIR, ¹³C NMR, TGA, and XRD analyses.

Characterization of CS

Scanning electron microscopy (SEM)

The morphological features of the CS were determined by scanning electron microscopy (SEM) with a JEOL JCM-6000 scanning electron microscope at an acceleration voltage of 15 kV. Before the analysis, the samples were coated with gold.

Attenuated total reflection–Fourier transform infrared spectroscopy (ATR–FTIR)

The ATR-FTIR spectroscopy analysis of the CS was performed with an FTIR spectrometer (Nicolet IS50) with a single-reflection ATR and type-IIA diamond crystal mounted on tungsten carbide. The diamond ATR had a sampling area of approximately 0.5 mm², and a consistent reproducible pressure was applied to every sample. The ATR-FTIR spectra were collected at 4 cm⁻¹ resolution with 64 scans. Each spectrum corresponds to five averaged spectra, and all spectra were corrected with the advanced ATR correction of OMNIC 9 to eliminate the diamond crystal effect and enable a comparison with the transmission spectra.

The ATR-FTIR spectroscopy analysis of the CSNC films was performed by following the same procedure as that for the CS.

Table 1 Chemical composition of cocoa shell

Component	Value	Method
Moisture (wt%)	2.6 ± 0.3	AOAC 931.04 (Official Methods of Analysis of AOAC INTERNATIONAL 2002)
Crude fat (wt%)	1.8 ± 0.1	AOAC 920.39 (Official Methods of Analysis of AOAC INTERNATIONAL 2002)
Total fat (wt%)	3.6 ± 0.9	AOAC 922.06 (Official Methods of Analysis of AOAC INTERNATIONAL 2002)
Cellulose (wt%)	27.7	AOAC 973.18, AOAC 2002:04 (Official Methods of Analysis of AOAC INTERNATIONAL 2002)
Hemicelluloses (wt%)	11.1	AOAC 973.18, AOAC 2002:04 (Official Methods of Analysis of AOAC INTERNATIONAL 2002)
Lignin (wt%)	15.6	AOAC 973.18, AOAC 2002:04 (Official Methods of Analysis of AOAC INTERNATIONAL 2002)

Characterization of CSNC

Moisture and crude fat

To determine the moisture of the CSNC films, 3.0 ± 0.2 g of the sample was treated in a conventional oven at 100 ± 5 °C for 3–4 h and dried to a constant weight (Association of Analytical Chemists Inc 2002). The crude fat content was determined according to the AOAC Official Method 963.15. After the moisture determination, the CS fat was extracted with hexane for 6 h with a Soxhlet apparatus. The crude fat content was determined as the difference between the weights of the dried samples before and after the extraction.

CP/MAS ^{13}C nuclear magnetic resonance (^{13}C NMR)

The ^{13}C NMR solid-state spectrum was recorded with a Bruker 400 WB Plus spectrometer at room temperature, and the spectra were collected with a 4 mm CP/MAS probe at 10,000 Hz. The CP/MAS ^{13}C NMR spectra of the solid samples were collected for 12 h with the standard pulse sequence at 100.6 MHz, a time domain of 2 K, spectral width of 29 kHz, contact time of 1.5 ms, and inter-pulse delay of 5 s at 25 °C.

X-ray diffraction (XRD)

The samples were X-rayed with the Panalytical X'Pert Pro MPD equipment with Ni-filtered Cu $K\alpha 1$ radiation ($\lambda = 1.540$ nm) at 40 kV and 40 mA. The data were collected in the reflection mode at a diffraction angle 2θ from 10° to 40° in steps of 0.026° .

Crystallinity index (CrI) calculation

The CrI of the CSNC films was determined by three different methods with ATR–FTIR, ^{13}C NMR, and XRD. The FTIR method (also known as “Nelson and O’Connor method”) uses the ratio between the bands at 1372 and 2900 cm^{-1} to determinate the total CrI (Nelson and O’Connor 1964a, b). The ^{13}C NMR C4 peak separation or Newman method uses the peak at 89 ppm (C4 carbon in ordered cellulose structures) and the peak at 84 ppm (C4 carbon of disordered cellulose). Moreover, the CrI was calculated by dividing the area of the crystalline peak (integrating

the peak from 87 to 93 ppm) by the total area assigned to the C4 peaks (integrating the region from 80 to 93 ppm) (Newman 2004). Finally, in the XRD Seagal method, the CrI was calculated based on the height ratio of the intensity of the crystalline peak ($I_{200} - I_{Am}$) and total intensity (I_{200}) after subtracting the background signal measured without the cellulosic sample (French 2014).

Fluorescent microscopy

The fat and cellulose phases in the CSNC suspension were investigated by fluorescence microscopy (Zeiss Axio Observer, Zeiss, Germany) with $10\times$ and $63\times$ oil immersion objectives. In the sample preparation, 1 mL nanocellulose was stained with 8 μL Nile red (for the oil phase) and then with 6 μL of Calcofluor white (for the cellulose nanofibers); 4 μL of the prepared samples was used for the study (Bai et al. 2019a, b).

Atomic force microscopy (AFM)

The morphology of the CSNC was studied with AFM. The samples were imaged in the tapping mode with a Nanoscope IIIa microscope (MultimodeTM Digital Instruments) with a multimode head at 180 kHz. In addition, a cantilever of 125 mm length and 5–10 nm tip radius was used. The nanocellulose samples were diluted in distilled water and sonicated (Ultrasons P-Selecta sonicator) at room temperature to achieve a good dispersion of the nanocellulose. Subsequently, a fine layer of the sample was deposited on a mica substrate with a spin-coater (2 min at 2000 rpm). Before the morphological analysis, the samples were stored in a vacuum desiccator for three days.

Results and discussion

To determine the CS morphology, a longitudinal section of the sample was studied by SEM before the milling procedure. As shown in Fig. 1a and b, sclerenchyma cells fibers, and tracheid elements are observed (Dickison 2000). Furthermore, a tracheid element is a type of xylem conductive cell through which plant nutrients can circulate, was found next to sclerenchyma cells fibers (Dickison 2000). The

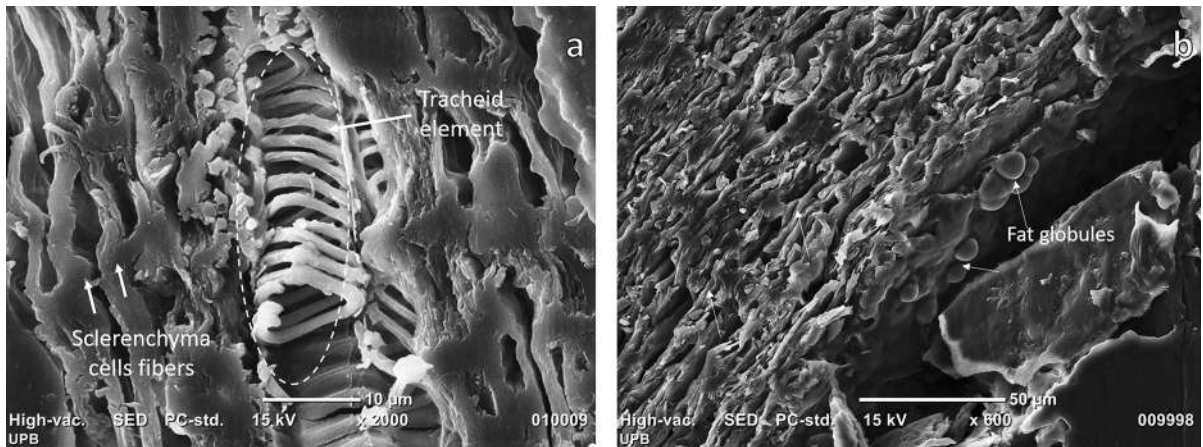


Fig. 1 SEM images of cocoa shell: **a** longitudinal section cut showing elementary fiber and tracheid, **b** longitudinal section cut showing elementary fiber and fat globules; inset of each figure shows digital images of sample

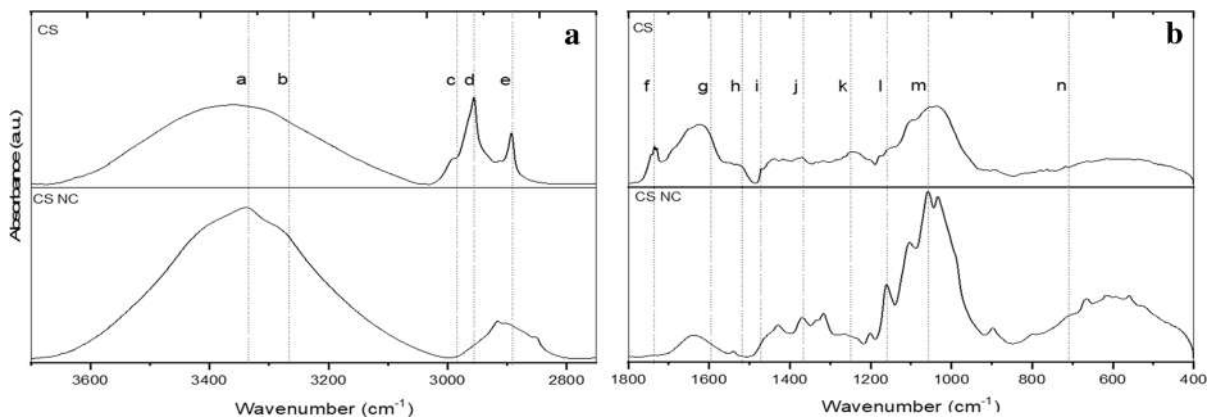


Fig. 2 ATR-FTIR spectra of cocoa shell and cocoa shell nanocellulose films for **a** 3700–2800 cm^{-1} and **b** 1800–400 cm^{-1}

sclerenchyma cells fibers and tracheid element have a cell wall (composite material), where semi-crystalline components (cellulose) interact with the amorphous matrix; its major components are hemicelluloses and lignin (Table 1) (Gañán et al. 2004; Gañán et al. 2008; Gorshkova et al. 2010).

As shown in Table 1, the CS is also composed of fat. In vegetable materials, it resides inside the cell or is deposited on vegetable tissues in the form of fat globules (arrows in Fig. 2b). The cell wall encloses several structures composed of different biomolecules; one of these are triacylglycerides, which are confined to discrete spherical organelles (oil bodies),

which consist of a triglyceride matrix surrounded by a monolayer of phospholipids linked together by proteins (Passos et al. 2009). In both cases, the fat is bonded to proteins (hydrogen bonds, covalent bonds), carbohydrates (covalent bonds), and other lipids (covalent bonds and van der Waals interaction) (Dominguez et al. 1994).

Moreover, ATR-FTIR was used to complement the information obtained by SEM and determine the chemical structures in the CS. The vegetable fat, lignin, hemicellulose, and cellulose in the CS determined by ATR-FTIR are listed in Fig. 2, and Table 2 summarizes the main vibrations of the CS and CSNC

Table 2 Characteristic bands in ATR–FTIR spectra of cocoa shell and cocoa shell nanocellulose and their assignments according to literature

Wavenumber (cm ⁻¹) ^a	Group ^{**}	Band assignment	Cell component	Reference
^a 3335	O–H	O(3)H...O(5) intramolecular hydrogen bonds in cellulose	Cellulose	(Popescu et al. 2007)
^b 3285	O–H	O(6)H...O(3) intermolecular hydrogen bonds in cellulose	Cellulose	(Popescu et al. 2007)
^c 2953	C–H	Asymmetric stretching of aliphatic –CH ₃ in fatty acids	Triacylglycerides of vegetable fat	(Safar et al. 1994)
^d 2922	C–H	Symmetric stretching of aliphatic –CH ₂ in fatty acids	Triacylglycerides of vegetable fat	(Safar et al. 1994; Che Man et al. 2005)
^e 2853	C–H	Symmetric stretching of aliphatic –CH ₂ in fatty acids and lignin	Triacylglycerides of vegetable fat and lignin	(Safar et al. 1994; Che Man et al. 2005)
^f 1743	C = O	vibrations of acetyl and uronic ester groups of hemicelluloses or ester linkage of fatty acid and carboxylic group of the ferulic and p-coumaric acids of lignin	Hemicelluloses and lignin	(Safar et al. 1994; Che Man et al. 2005)
^g 1590	C = C	C = C stretching of the aromatic ring (S)	Lignin	(Popescu et al. 2007)
^h 1510	C = C	C = C stretching of the aromatic ring (G)	Lignin	(Popescu et al. 2007)
ⁱ 1462	C–H	Scissoring of aliphatic –CH ₂ in fatty acids	Triacylglycerides of vegetable fat	(Safar et al. 1994; Che Man et al. 2005)
^j 1377	C–H	Symmetric deformation of aliphatic –CH ₃ in fatty acids	Triacylglycerides of vegetable fat	(Safar et al. 1994)
^k 1235	C–O	Syringyl ring breathing and C–O stretching in lignin and xylan	Hemicelluloses and lignin	(Safar et al. 1994; Popescu et al. 2007)
^l 1162	C–O–C	C–O–C asymmetric stretching in cellulose I and cellulose II	Cellulose	(Popescu et al. 2007)
^m 1043	C–O–C	stretching of C–O–C in xylans associated with hemicelluloses and cellulose	Hemicelluloses and cellulose	(Safar et al. 1994; Popescu et al. 2007)
ⁿ 711		Iβ cellulose	Cellulose	(Zuluaga et al. 2009)

^a superscripts represent locations in ATR–FTIR spectra in Fig. 2

^{**} vibrational modes are associate to components in cocoa shell and cocoa shell nanofibers according to literature

according to literature. ATR–FTIR spectroscopy is a suitable technique for determining the variations in chemical structures introduced by isolation treatments (Zuluaga et al. 2009). The changes introduced by the chemical and mechanical treatments were evaluated by comparing four regions: (1) from 3600 to 3000 cm⁻¹, associated with OH stretching vibrations (hydrogen bonding pattern in cellulose; (Sugiyama et al. 1991b), (2) from 3000 to 2800 cm⁻¹, related to C–H vibrations in vegetable fat, cellulose, and lignin (Marchessault et al. 1960; Safar et al. 1994; Zuluaga

et al. 2009), (3) from 1500 to 1200 cm⁻¹, associated with CH₂ wagging and COH in-plane bending (Sugiyama et al. 1991a), and (4) from 1180 to 800 cm⁻¹, related to polysaccharides (Velásquez-Cock et al. 2016).

Several absorbance peaks related to the functional groups in lignin (^e2853 cm⁻¹, ^g1590 cm⁻¹, ^h1510 cm⁻¹, and ^k1235 cm⁻¹) decreased significantly after the chemical and mechanical treatments. In addition, the vibration at ^f1743 cm⁻¹ related to hemicelluloses functional groups decreased; nevertheless, it is still

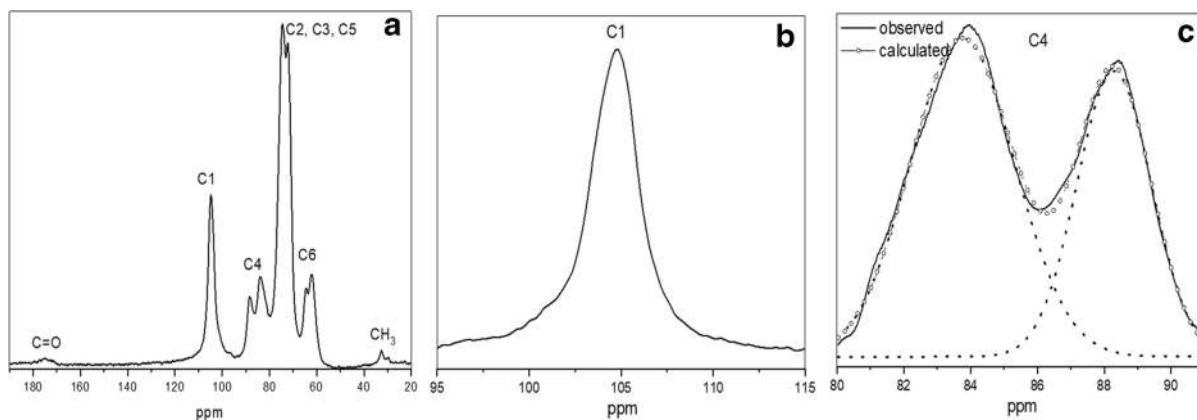


Fig. 3 (a) Solid-state CP/MAS ^{13}C NMR spectrum of cocoa shell nanocellulose; (b) parts of spectra from 95 to 115 ppm and (c) 80 to 92 ppm

observable in the CSNC spectrum. Several researchers have related this band to the presence of hemicelluloses after an alkali treatment because it has different mechanisms through which it binds to cellulose (Zuluaga et al. 2009). Hemicelluloses is one of the most difficult components to remove from cell walls owing to its strong interaction with cellulose (Zuluaga et al. 2009; Gorshkova et al. 2010; Velásquez-Cock et al. 2016). It could be physically interwoven into the cell wall (easily extractable by treatments with xyloglucanendoglucanase), form hydrogen bonds with polymers (extracted by alkali), or be tightly bonded to nanocellulose (extractable by treatments with cellulase) (Zuluaga et al. 2009; Gorshkova et al. 2010). This suggests that the isolation treatment possibly cleaved the two first types of interactions between xyloglucans and cellulose.

The ATR-FTIR spectra of the CSNC films in Fig. 2a and b exhibit the characteristic peaks of cellulose. The OH stretching vibrations occur at $3000\text{--}3650\text{ cm}^{-1}$, and the peaks at a3335 and $^b3285\text{ cm}^{-1}$ are related to $\text{O}(6)\text{H}\dots\text{O}(3)$ intermolecular bonding (Popescu et al. 2007). The vibrations at a3335 and $^b3285\text{ cm}^{-1}$ in the CSNC are increased compared to those in CS. As mentioned in the previous paragraph, the chemical treatment partially eliminated the non-cellulosic components lignin and hemicellulose, thereby enhancing the intermolecular interactions between the cellulose chains (Popescu et al. 2007; Zuluaga et al. 2009). In addition, the absorption band at $^n711\text{ cm}^{-1}$ is related to I_β cellulose (Fig. 2b).

Thus, the isolated cellulosic samples are rich in I_β phase (Zuluaga et al. 2009).

Figure 2a and b show that the CSNC films exhibit several vibrations that are related to functional groups of the main components of vegetable shell fat (oleic, palmitic, and capric fatty acids) (El-Saied et al. 1981). In addition, vibrations at $^c2953\text{ cm}^{-1}$, $^d2922\text{ cm}^{-1}$, $^e2853\text{ cm}^{-1}$, $^f1462\text{ cm}^{-1}$, and $^g1377\text{ cm}^{-1}$ were observed (Safar et al. 1994; Che Man et al. 2005). Hence, the cell wall cleavage promotes the liberation of other components, for instance triacylglycerides. The modification of cell wall polymers (e.g., pectic polysaccharides and hemicelluloses) increases the extraction of oil or fat in grape seed (Passos et al. 2009), almonds (Femenia et al. 2001), olives, avocados, and coconuts (Domínguez et al. 1994). To separate fats from vegetable tissues, several treatments with organic solvents, enzymes, or acid hydrolysis are required because of the complex interactions between fats, polysaccharides, and other biomolecules (Passos et al. 2009). Finally, the ATR-FTIR spectra of the CSNC films indicate that the chemical and mechanical treatments partially removed hemicelluloses and lignin (the CSNC film is a cellulosic sample with fat ($7.81 \pm 1.8\text{ wt}\%$) and hemicelluloses content).

Furthermore, functional groups of fatty acids, hemicelluloses, and cellulose were identified by ^{13}C NMR. Figure 3a shows the solid-state ^{13}C NMR spectrum of the CSNC film. The spectrum is dominated by signals associated with cellulose: C1, anomeric carbon: 104.71 ppm; C4: 88.43 ppm; C4: 83.79 ppm; cluster C2–C3–C5: 80–69 ppm; C6:

64.65 ppm; C6: 61.91 ppm (Newman 1997, 2004). Figure 3b shows that the C1 region is dominated by a signal at 104.7 ppm, which is primarily related to the I_{β} form of cellulose. Hence, the isolated cellulosic sample is I_{β} phase-rich (Newman 1997), as confirmed by the ATR–FTIR results (Fig. 2).

The other components (e.g., hemicelluloses and fat) show weaker signals than cellulose. The weak signal at approximately 175 ppm in Fig. 3a contains all the peaks generated from carboxyl carbons of fatty acids or hemicelluloses (Pollesello et al. 1996). In particular, the carboxyl groups of fatty acids generated peaks at 173.2 and 173.1 ppm (Pollesello et al. 1996). Other researchers have reported that the signals at 171 ppm are related to carboxylic carbons of acetyl groups attached to hemicelluloses, and a similar signal has been observed in the ^{13}C NMR spectrum of cellulose from a silver tree fern (*Cyathea dealbata*), thereby indicating the presence of hemicelluloses. The other signals of methyl and methylene carbons of oleic acid occur at 32.61 ppm (Seino et al. 1984). As previously

mentioned, oleic acid is the principal fatty acid in CS fat (El-Saied et al. 1981).

Both ATR–FTIR and solid-state ^{13}C NMR results were used to determine the dominant crystalline structure of the isolated cellulose (I_{β}). The XRD pattern of the CSNC film presented in Fig. 4 is similar to that of laterally disordered cellulose I_{β} (Chanzy et al. 1978; Zuluaga et al. 2009) because of the general aspect of the spectra and, in particular, the overlap of $1\bar{1}0$ and 110 reflections. The peak at the lowest angle can be described as the overlap of $1\bar{1}0$ and 110 reflections, and 102, 200, and 004 reflections occur with increasing diffraction angle (Sugiyama et al. 1991c).

The CrI in Table 3 is one of the most important crystalline structure parameters. It is commonly used to quantify the amount of crystalline cellulose in cellulosic materials and to interpret changes in the cellulose structures after physicochemical and biological treatments. However, the CrI varies significantly depending on the measurement method because each method evaluates crystalline and less-ordered materials differently (Evans et al. 1995). For example, the XRD Segal and ^{13}C NMR methods are sensitive to the long- and short-range order, respectively, while the FTIR method is sensitive to the short-range order and composition (Evans et al. 1995). In addition, solid-state ^{13}C NMR and FTIR spectroscopy determine the CrI and the XRD Segal method the crystallinity percentage (Nelson and O'Connor 1964b; Newman 2004). Nevertheless, the three methods exhibit excellent correlation (Evans et al. 1995).

Choosing the technique that provides the most accurate evaluation of the cellulose crystallinity is not trivial. As shown in Table 3, the Nelson and O'Connor method results in the lowest CrI. This method provides only relative values because the spectrum always contains contributions from different sample components. Therefore, for cellulose with a significant content of fat as CSNC film, the band at 2900 cm^{-1}

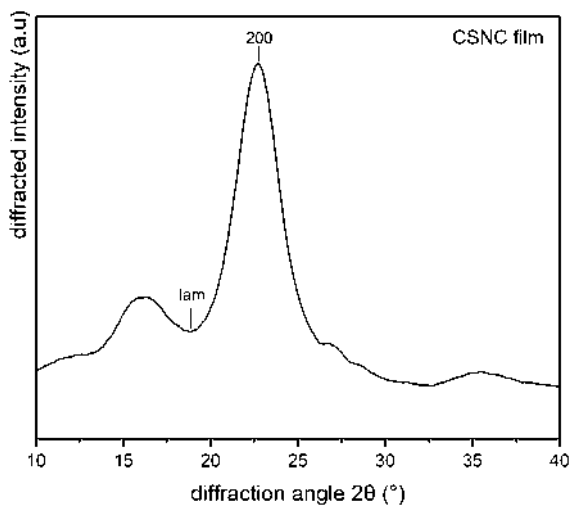


Fig. 4 XRD profiles of cocoa shell nanocellulose film. The indexation is based on Sugiyama et al. (1991c)

Table 3 Crystallinity index of cocoa shell nanocellulose film determined by different methods

Method	Crystallinity index (CrI)	Technique	Reference
Nelson and O'Connor	0.45	ATR–FTIR	(Nelson and O'Connor 1964a, b)
Newman	0.65	^{13}C NMR	(Newman 2004)
XRD Segal	71.36%	XRD	(Park et al. 2010)

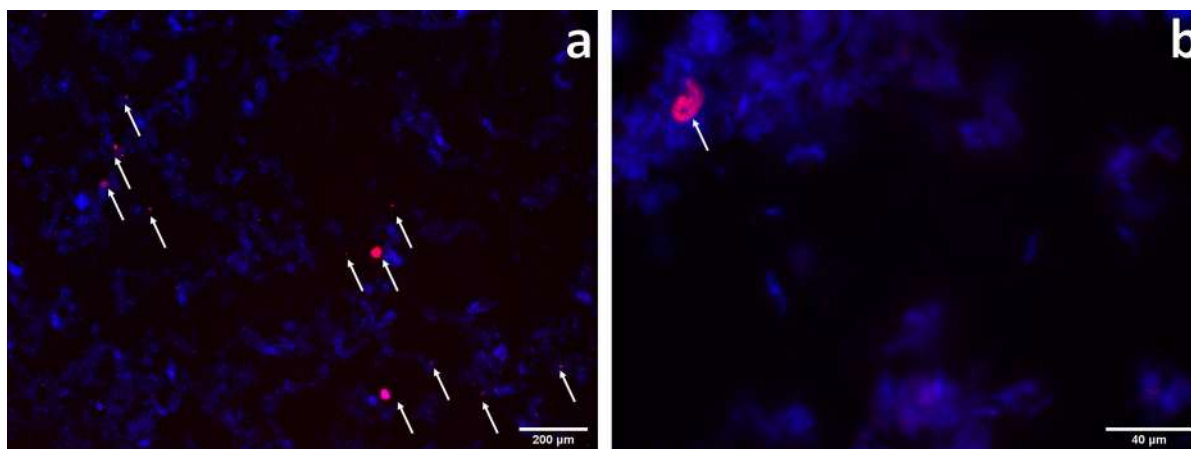


Fig. 5 Fluorescence micrographs of cocoa shell nanocellulose suspension at (a) 100 × and (b) 630 × magnifications. The white arrows indicate the presence of fat particles. Before the

is also associated with the symmetric or asymmetric stretching vibrations of aliphatic $-CH_3$ and $-CH_2$ in fatty acids (Safar et al. 1994; Che Man et al. 2005). These can mask the results of the Nelson and O'Connor method (Poletto et al. 2014; Ornaghi et al. 2014).

The CrI determined by the Newman method uses the C4 peak cluster, which is only assigned to carbon in ordered cellulose structures. Therefore, the functional groups of fat do not affect this method. Thus, the most suitable methods for determining the CrI of cellulosic samples from CS are the Newman and XRD deconvolution methods. Additional treatments for removing non-cellulosic components and fat can be implemented; however, they can change the structure of the cellulosic sample and reduce its crystallinity (Zuluaga et al. 2009). Literature provides the CrI of cellulosic samples with various compositions of polysaccharides (Nelson and O'Connor 1964a, b; Park et al. 2010). However, no publication that provided the CrI of cellulose samples with vegetable fat was found.

Furthermore, fluorescent microscopy was used to study the distribution of cellulose and vegetable fat in the samples. This technique has been commonly used to identify nanofibers and oily phases on Pickering emulsions with nanocellulose or nanocellulose whiskers (Bai et al. 2018, 2019b). As shown in Fig. 5a and b, when the sample is illuminated with fluorescent light, the stained cellulosic material (blue) and vegetable fat (red) appear as two different components in the sample (cellulosic component exhibits higher

investigation, the oil phase was stained with Nile red and the cellulosic components with Calcofluor white

percentage). Cellulose is hydrophilic; therefore, it presents a lower compatibility with lipids and fats. However, as shown in Fig. 5a, the suspension is homogeneous.

According to Fig. 5a, the cellulosic components and vegetable fat do not form separated phases; they are homogeneously distributed. Cellulose can stabilize oil in water emulsions because it interacts directly with the fat structures, thereby forming Pickering emulsions (Winuprasith and Suphantharika 2013, 2015; Cunha et al. 2014). The fluoresce images do not show any evidence of an emulsion. However, owing to the large aspect ratio, the CSNC forms an entangled three-dimensional network that traps fat globules, as shown in Fig. 5b (Cunha et al. 2014; Velásquez-Cock et al. 2019). Other authors have reported that, cellulose is an excellent suspension medium for other solids and an emulsifying base for organic liquids, for example, oil/water emulsions (Turbak et al. 1983; Winuprasith and Suphantharika 2013, 2015; Cunha et al. 2014; Bai et al. 2018).

The entangled network formed by the CSNC is clearly visible in the AFM images in Figs. 6a and b. The cellulosic material isolated from the CS is nanocellulose with fibrillar morphology (diameters below 100 nm). In addition, nanofibers with diameters between 30 and 80 nm and lengths of few micrometers can be seen. Hence, the chemical and mechanical treatments promoted the fibrillation process.

Overall, the results indicate that a suspension of nanocellulose, hemicelluloses, and fat (i.e., a

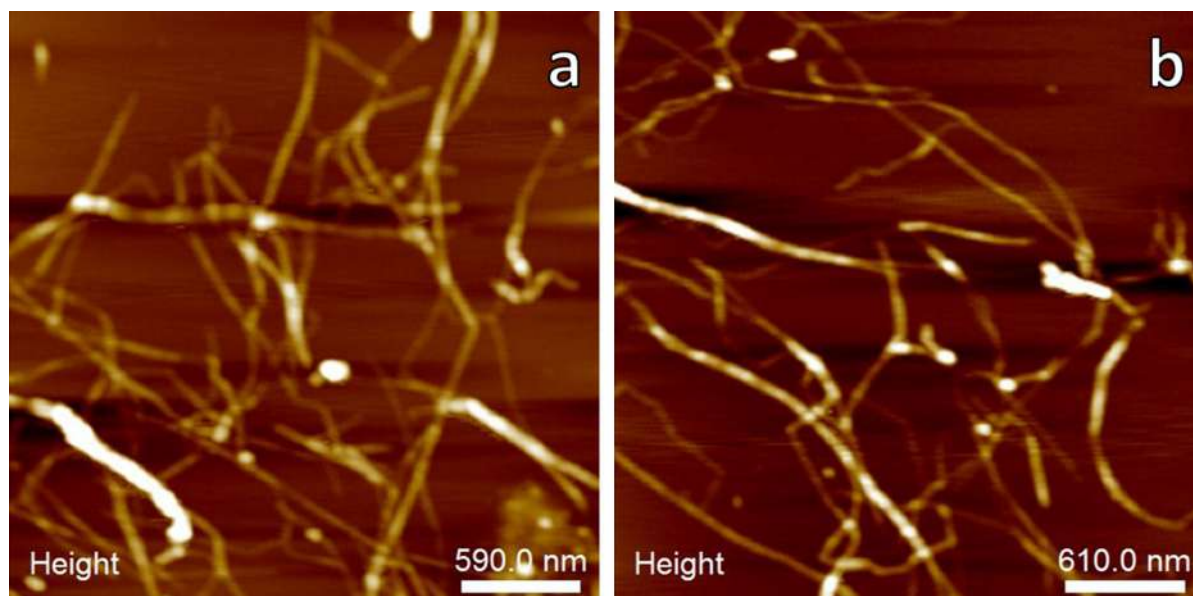


Fig. 6 AFM height images of cocoa shell nanocellulose film

holocellulose nanofibers and fat suspension) can be isolated from CS by chemical and mechanical treatments. This process deconstructs the cell wall into holocellulose nanofibers. The result is an entangled network, which stabilizes CS fat. Thus, the by-product from the cocoa industry can be used to produce suspensions of holocellulose nanofibers for the food industry. For example, CSNC can be used as a natural emulsifying and stabilizing ingredient. Because of the similarities between cocoa fat and CS fat (El-Saied et al. 1981; Okiyama et al. 2017), this new material is an interesting candidate for the enrichment of food products, such as salad dressings, chocolate, whipped toppings, sauces, foams, soups, puddings, dips, and ice cream (Mizuguchi et al. 1983; Turbak et al. 1983; Gómez et al. 2016; Velásquez-Cock et al. 2019).

Conclusions

In this study, chemical and mechanical treatments were used to isolate a suspension of holocellulose nanofibers and fat from CSs. The chemical and crystalline structures of the isolated sample were evaluated by ATR–FTIR, ^{13}C NMR, and XRD. The ATR–FTIR results confirm the partial removal of non-cellulosic components and CS fat. The resistance of non-cellulosic components to the extraction with

alkali might be due to their strong bonds. According to the FTIR–ATR and ^{13}C NMR results, the isolated holocellulose nanofibers contains significant amounts of fat (7.81 ± 1.8 wt%) because the isolation process promoted its liberation. The ATR–FTIR, ^{13}C NMR, and XRD spectra contain reflections associated with cellulose I_β . The most adequate methods for calculating the CrI of this sample kind with fat content are the XRD deconvolution and ^{13}C NMR C4 separation methods. Moreover, the fluorescence microscopy results confirm the formation of a suspension, and the AFM results show that the isolated holocellulose nanofibers has a large aspect ratio, which promoted the formation of an entangled network that stabilizes fat.

The presence of fat in the suspension enables a broader application of holocellulose nanofibers and fat suspensions in the food industry. They can be used as ingredients for food products enriched with CS fat, such as salad dressings, whipped toppings, sauces, foams, soups, puddings, dips, and ice cream.

Acknowledgments The authors acknowledge the financial support from the Research Center for Investigation Development (CIDI) from the Universidad Pontificia Bolivariana (Project No. 092C-05/18–49), NANOCELIA Network of the Iberoamerican Program of Science and Technology for Development (CYTED), Administrative Department for Science, Technology and Innovation of the

Colombian Government (COLCIENCIAS), and *Compañía Nacional de Chocolates*.

References

- Bai L, Huan S, Xiang W, Rojas OJ (2018) Pickering emulsions by combining cellulose nanofibrils and nanocrystals: phase behavior and depletion stabilization. *Green Chem* 20:1571–1582. <https://doi.org/10.1039/C8GC00134K>
- Bai L, Lv S, Xiang W et al (2019a) Oil-in-water Pickering emulsions via microfluidization with cellulose nanocrystals: 1 Formation and stability. *Food Hydrocoll* 96:699–708. <https://doi.org/10.1016/j.foodhyd.2019.04.038>
- Bai L, Lv S, Xiang W et al (2019b) Oil-in-water Pickering emulsions via microfluidization with cellulose nanocrystals: 2 vitro lipid digestion. *Food Hydrocoll* 96:709–716. <https://doi.org/10.1016/j.foodhyd.2019.04.039>
- Bonvehí JS, Jordà RE (1998) Constituents of cocoa husks. *Zeitschrift Fur Naturforsch-Sect C J Biosci* 53:785–792. <https://doi.org/10.1515/znc-1998-9-1002>
- Campos-Vega R, Nieto-Figueroa KH, Oomah BD (2018) Cocoa (*Theobroma cacao* L.) pod husk: renewable source of bioactive compounds. *Trends Food Sci Technol* 81:172–184. <https://doi.org/10.1016/j.tifs.2018.09.022>
- Chanzy H, Imada K, Vuong R (1978) Electron diffraction from the primary wall of cotton fibers. *Protoplasma* 94:299–306. <https://doi.org/10.1007/BF01276778>
- Che Man YB, Syahariza ZA, Mirghani MES et al (2005) Analysis of potential lard adulteration in chocolate and chocolate products using Fourier transform infrared spectroscopy. *Food Chem* 90:815–819. <https://doi.org/10.1016/j.foodchem.2004.05.029>
- Cunha AG, Mougél J-B, Cathala B et al (2014) Preparation of double pickering emulsions stabilized by chemically tailored nanocelluloses. *Langmuir* 30:9327–9335. <https://doi.org/10.1021/la5017577>
- Dickinson E (2012) Use of nanoparticles and microparticles in the formation and stabilization of food emulsions. *Trends Food Sci Technol* 24:4–12. <https://doi.org/10.1016/j.tifs.2011.09.006>
- Dickison WC (2000) *Integrative plant anatomy*. San Diego
- Domínguez H, Núñez MJ, Lema JM (1994) Enzymatic pretreatment to enhance oil extraction from fruits and oilseeds: a review. *Food Chem* 49:271–286. [https://doi.org/10.1016/0308-8146\(94\)90172-4](https://doi.org/10.1016/0308-8146(94)90172-4)
- Donkoh A, Atuahene CC, Wilson BN, Adomako D (1991) Chemical composition of cocoa pod husk and its effect on growth and food efficiency in broiler chicks. *Anim Feed Sci Technol* 35:161–169. [https://doi.org/10.1016/0377-8401\(91\)90107-4](https://doi.org/10.1016/0377-8401(91)90107-4)
- El-Saied HM, Morsi MK, Amer MMA (1981) Composition of cocoa shell fat as related to cocoa butter. *Z Ernährungswiss* 20:145–151. <https://doi.org/10.1007/BF02021260>
- Evans R, Wallis AFA, Newman RH et al (1995) Changes in cellulose crystallinity during kraft pulping: comparison of infrared, x-ray diffraction and solid state nmr results. *Holzforschung* 49:498–504. <https://doi.org/10.1515/hfsg.1995.49.6.498>
- FAO (2019) Food and agriculture Organization of the United Nations. [https://www.fao.org/faostat/en/#search/Cocoa%2C beans](https://www.fao.org/faostat/en/#search/Cocoa%2C%20beans). Accessed 21 Nov 2019
- FEDECACAO (2019) No Title. <https://www.fedecacao.com.co/portal/index.php/es/2015-04-23-20-00-31/investigacion>. Accessed 22 Nov 2019
- Femenia A, García-Marín M, Simal S et al (2001) Effects of supercritical carbon dioxide (SC-CO₂) oil extraction on the cell wall composition of almond fruits. *J Agric Food Chem* 49:5828–5834. <https://doi.org/10.1021/jf010532e>
- French AD (2014) Idealized powder diffraction patterns for cellulose polymorphs. *Cellulose* 21:885–896. <https://doi.org/10.1007/s10570-013-0030-4>
- Gañán P, Zuluaga R, Cruz J et al (2008) Elucidation of the fibrous structure of Musaceae maturate. *Cellulose* 15:131–139. <https://doi.org/10.1007/s10570-007-9150-z>
- Gañán P, Zuluaga R, Velez JM, Mondragon I (2004) Biological natural retting for determining the hierarchical structuration of banana fibers. *Macromol Biosci* 4:978–983. <https://doi.org/10.1002/mabi.200400041>
- Gómez HC, Serpa A, Velásquez-Cock J et al (2016) Vegetable nanocellulose in food science: a review. *Food Hydrocoll* 57:178–186. <https://doi.org/10.1016/j.foodhyd.2016.01.023>
- Gorshkova TA, Mikshina PV, Gurjanov OP, Chemiksova SB (2010) Formation of plant cell wall supramolecular structure. *Biochem* 75:159–172. <https://doi.org/10.1134/S0006297910020069>
- Hemmati F, Jafari SM, Kashaninejad M, Barani Motlagh M (2018) Synthesis and characterization of cellulose nanocrystals derived from walnut shell agricultural residues. *Int J Biol Macromol* 120:1216–1224. <https://doi.org/10.1016/j.ijbiomac.2018.09.012>
- Jonoobi M, Oladi R, Davoudpour Y et al (2015) Different preparation methods and properties of nanostructured cellulose from various natural resources and residues: a review. *Cellulose* 22:935–969. <https://doi.org/10.1007/s10570-015-0551-0>
- Karim AA (2014) Antioxidant properties of cocoa pods and shells. *Malays Cocoa J* 8:49–56
- Lecumberri E, Mateos R, Izquierdo-Pulido M et al (2007) Dietary fibre composition, antioxidant capacity and physico-chemical properties of a fibre-rich product from cocoa (*Theobroma cacao* L.). *Food Chem* 104:948–954. <https://doi.org/10.1016/j.foodchem.2006.12.054>
- Lu F, Rodriguez-Garcia J, Van Damme I et al (2018) Valorisation strategies for cocoa pod husk and its fractions. *Curr Opin Green Sustain Chem* 14:80–88. <https://doi.org/10.1016/j.cogsc.2018.07.007>
- Marchessault RH, Pearson FG, Liang CY (1960) Infrared spectra of crystalline polysaccharides. *Biochim Biophys Acta* 45:499–507. [https://doi.org/10.1016/0006-3002\(60\)91486-4](https://doi.org/10.1016/0006-3002(60)91486-4)
- Martín-Cabrejas MA, Valiente C, Esteban RM et al (1994) Cocoa hull: a potential source of dietary fibre. *J Sci Food Agric* 66:307–311. <https://doi.org/10.1002/jsfa.2740660307>
- Mizuguchi K, Fujioka I, Kobayashi H (1983) Preparation of retort food
- Nelson ML, O'Connor RT (1964a) Relation of certain infrared bands to cellulose crystallinity and crystal latticed type.

- Part I. Spectra of lattice types I, II, III and of amorphous cellulose. *J Appl Polym Sci* 8:1311–1324. <https://doi.org/10.1002/app.1964.070080322>
- Nelson ML, O'Connor RT (1964b) Relation of certain infrared bands to cellulose crystallinity and crystal lattice type. part ii. a new infrared ratio for estimation of crystallinity in celluloses i and ii *. *J Appl Polym Sci* 8:1325–1341
- Newman RH (2004) Homogeneity in cellulose crystallinity between samples of *Pinus radiata* wood. *Holzforschung* 58:91–96. <https://doi.org/10.1515/HF.2004.012>
- Newman RH (1997) Crystalline forms of cellulose in the silver tree fern *Cyathea dealbata*. *Cellulose* 4:269–279. <https://doi.org/10.1023/A:1018496025143>
- Official Methods of Analysis of AOAC INTERNATIONAL (2002) 15th Edn, AOAC INTERNATIONAL, Gaithersburg, MD, USA, Official Method
- Okiyama DCG, Navarro SLB, Rodrigues CEC (2017) Cocoa shell and its compounds: Applications in the food industry. *Trends in Food Science & Technology* 63:103–112
- Ornaghi HL, Poletto M, Zattera AJ, Amico SC (2014) Correlation of the thermal stability and the decomposition kinetics of six different vegetal fibers. *Cellulose* 21:177–188. <https://doi.org/10.1007/s10570-013-0094-1>
- Park S, Baker JO, Himmel ME et al (2010) Cellulose crystallinity index: measurement techniques and their impact on interpreting cellulase performance. *Biotechnol Biofuels* 3:10. <https://doi.org/10.1186/1754-6834-3-10>
- Passos CP, Yilmaz S, Silva CM, Coimbra MA (2009) Enhancement of grape seed oil extraction using a cell wall degrading enzyme cocktail. *Food Chem* 115:48–53. <https://doi.org/10.1016/j.foodchem.2008.11.064>
- Poletto M, Ornaghi Júnior HL, Zattera AJ (2014) Native cellulose: structure, characterization and thermal properties. *Materials (Basel)* 7:6105–6119. <https://doi.org/10.3390/ma7096105>
- Poletto M, Zattera AJ, Forte MMC, Santana RMC (2012) Bioresource technology thermal decomposition of wood : influence of wood components and cellulose crystallite size. *Bioresour Technol* 109:148–153. <https://doi.org/10.1016/j.biortech.2011.11.122>
- Pollesello P, Eriksson O, Höckerstedt K (1996) Analysis of total lipid extracts from human liver by ¹³C and ¹H nuclear magnetic resonance spectroscopy. *Anal Biochem* 236:41–48. <https://doi.org/10.1006/abio.1996.0129>
- Popescu CM, Popescu MC, Singurel G et al (2007) Spectral characterization of eucalyptus wood. *Appl Spectrosc* 61:1168–1177. <https://doi.org/10.1366/000370207782597076>
- Safar M, Bertrand D, Robert P et al (1994) Characterization of edible oils, butters and margarines by Fourier transform infrared spectroscopy with attenuated total reflectance. *J Am Oil Chem Soc* 71:371–377. <https://doi.org/10.1007/BF02540516>
- Seino H, Uchibori T, Nishitani T, Inamasu S (1984) Enzymatic synthesis of carbohydrate esters of fatty acid (I) esterification of sucrose, glucose, fructose and sorbitol. *J Am Oil Chem Soc* 61:1761–1765. <https://doi.org/10.1007/BF02582144>
- Serra Bonvehí J, Ventura Coll F (1999) Protein quality assessment in cocoa husk. *Food Res Int* 32:201–208. [https://doi.org/10.1016/S0963-9969\(99\)00088-5](https://doi.org/10.1016/S0963-9969(99)00088-5)
- Souza LO, Lessa OA, Dias MC et al (2019) Study of morphological properties and rheological parameters of cellulose nanofibrils of cocoa shell (*Theobroma cacao* L.). *Carbohydr Polym* 214:152–158. <https://doi.org/10.1016/j.carbpol.2019.03.037>
- Ström G, Öhgren C, Ankerfors M (2013) Nanocellulose as an additive in foodstuff. pp 1–28
- Sugiyama J, Persson J, Chanzy H (1991a) Combined infrared and electron diffraction study of the polymorphism of native celluloses. *Macromolecules* 24:2461–2466. <https://doi.org/10.1021/ma00009a050>
- Sugiyama J, Vuong R, Chanzy H (1991b) Electron diffraction study on the two crystalline phases occurring in native cellulose from an algal cell wall. *Macromolecules* 24:4168–4175. <https://doi.org/10.1021/ma00014a033>
- Sugiyama J, Vuong R, Chanzy H (1991c) Electron diffraction study on the two crystalline phases occurring in native cellulose from an algal cell wall. *Macromolecules* 24(14):4168–4175
- Sun JX, Sun XF, Zhao H, Sun RC (2004) Isolation and characterization of cellulose from sugarcane bagasse. *Polym Degrad Stab* 84:331–339. <https://doi.org/10.1016/j.polyimdegradstab.2004.02.008>
- Turbak AF, Snyder FW, Sandberg KR (1983) Microfibrillated cellulose, a new cellulose product: Properties, uses, and commercial potential. *J Appl Polym Sci Appl Polym Symp* 37:815–827
- Velásquez-Cock J, Gañán P, Posada P et al (2016) Influence of combined mechanical treatments on the morphology and structure of cellulose nanofibrils: thermal and mechanical properties of the resulting films. *Ind Crops Prod* 85:1–10. <https://doi.org/10.1016/j.indcrop.2016.02.036>
- Velásquez-Cock J, Serpa A, Vélez L et al (2019) Influence of cellulose nanofibrils on the structural elements of ice cream. *Food Hydrocoll* 87:204–213. <https://doi.org/10.1016/j.foodhyd.2018.07.035>
- Winuprasith T, Suphantharika M (2015) Properties and stability of oil-in-water emulsions stabilized by microfibrillated cellulose from mangosteen rind. *Food Hydrocoll* 43:690–699. <https://doi.org/10.1016/j.foodhyd.2014.07.027>
- Winuprasith T, Suphantharika M (2013) Microfibrillated cellulose from mangosteen (*Garcinia mangostana* L.) rind: preparation, characterization, and evaluation as an emulsion stabilizer. *Food Hydrocoll* 32:383–394. <https://doi.org/10.1016/j.foodhyd.2013.01.023>
- Zuluaga R, Putaux JL, Cruz J et al (2009) Cellulose microfibrils from banana rachis: effect of alkaline treatments on structural and morphological features. *Carbohydr Polym* 76:51–59. <https://doi.org/10.1016/j.carbpol.2008.09.024>

Publisher's Note Springer Nature remains neutral with regard to jurisdictional claims in published maps and institutional affiliations.